

INFORMATION TO USERS

This dissertation copy was prepared from a negative microfilm created and inspected by the school granting the degree. We are using this film without further inspection or change. If there are any questions about the content, please write directly to the school. The quality of this reproduction is heavily dependent upon the quality of the original material.

The following explanation of techniques is provided to help clarify notations which may appear on this reproduction.

1. Manuscripts may not always be complete. When it is not possible to obtain missing pages, a note appears to indicate this.
2. When copyrighted materials are removed from the manuscript, a note appears to indicate this.
3. Oversize materials (maps, drawings and charts are photographed by sectioning the original, beginning at the upper left hand corner and continuing from left to right in equal sections with small overlaps.

UMI[®]


ProQuest Information and Learning
300 North Zeeb Road, Ann Arbor, MI 48106-1346 USA
800-521-0600


STUDY OF THE PLASMA ARC BEHAVIOR DURING
VARIABLE POLARITY PLASMA ARC WELDING
USING THE SPLIT ANODE METHOD

RICHARD ETHAN MARQUES

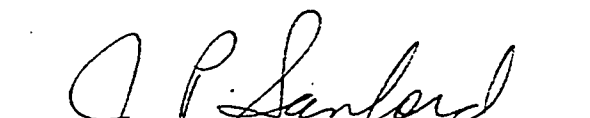
Department of Metallurgical and Materials Engineering

APPROVED:


Dr. John C. McClure, Chair


Dr. Roy M. Arrowood


Dr. Miguel Picornell


Associate Vice President for
Research and Graduate Studies

PREVIEW

*For God so loved the world that he gave his one and only
Son, that whoever believes in him shall not perish
but have eternal life.*

John 3:16

STUDY OF THE PLASMA ARC BEHAVIOR DURING
VARIABLE POLARITY PLASMA ARC WELDING
USING THE SPLIT ANODE METHOD

by

RICHARD ETHAN MARQUES, B.S.MET.E.

THESIS

Presented to the Faculty of the Graduate School of

The University of Texas at El Paso

in Partial Fulfillment

of the Requirements

for the Degree of

MASTER OF SCIENCE

Department of Metallurgical and Materials Engineering

THE UNIVERSITY OF TEXAS AT EL PASO

July 1994

ACKNOWLEDGEMENTS

Thanks to Dr. John McClure, Dr. Roy Arrowood and Dr. Miguel Picornell for serving on my thesis committee. Thanks to Dr. McClure in particular for allowing me to pursue this study. Thanks to Dr. Art Nunes and NASA Marshall Space Flight Center in Huntsville, Alabama for support during my graduate studies and also to the Patricia Roberts Harris Fellowship--all financial support is gratefully acknowledged.

Special thanks to the VPPA welding group including Carlos Rincon, Kevin Hamann, Haihui Hou, Shane Andrews, Luis F. Martinez, Tonghui Pang, Qingdong Pang, and Gabriel Garcia. To Cathy Buttz-- thanks for your help, inquisitive mind, compelling conversation and youthful spirit.

Thanks to Faye Eckberg, Juanita Borunda, Cynthia Trujillo, Cecilia Dale and Humberto Amaro for their help in moving my project along to completion.

Fellow grad students (too numerous to acknowledge on this tiny piece of paper) have been very helpful with advice, stress-relieving activities and hearty fellowship--thanks!!

Thanks to my family--to my wonderful children for making all these school days even more memorable and the nights eventful! --to my wife for supporting me with her time, her patience and her love during my graduate studies.

Finally, I give thanks to GOD for his love and his word!

Thesis submitted to committee on June 30, 1994.

ABSTRACT

In any arc welding process, it is important to know the current density distribution around the arc as this is primarily responsible for the energy needed to melt the metal. Numerous studies have been performed on gas tungsten arcs to determine the current density distribution around the arc under various conditions but similar studies have not been made on a variable polarity plasma arc.

The split anode method was used to study DCEN arcs and variable polarity plasma arcs to determine how the arc widths change as functions of welding mode, welding current and shield gas composition. Photographs of the arc were made to visualize the changes in the arc. For the current range studied, an electromagnetic "pinch effect" was found to influence the arc unless a counterbalancing kinetic force was present. DCEN arcs are larger than comparable VPPA arcs. Shield gas composition effects on the arc were not distinct.

TABLE OF CONTENTS

Acknowledgements	iv
Abstract	v
Table of Contents	vi
List of Tables	ix
List of Figures	x
Chapter 1: Introduction	1
1.1 Welding Aluminum	1
1.2 Gas Tungsten Arc Welding	3
1.3 Plasma Arc Welding	4
1.4 Variable Polarity Plasma Arc Welding	7
1.5 DCEP Cleaning Mechanism	12
1.5.1 Ion Sputtering Mechanism	12
1.5.2 Dielectric Breakdown Mechanism	13
1.6 Current Distribution Measurements	18
1.7 Summary	26
Chapter 2: Experimental Procedures	27
2.1 Welder Set-Up	27
2.2 Copper Anodes	35

2.3 Anode and Torch Alignment	40
2.4 Hardware Configuration	42
2.5 Data Collecting	47
2.6 Data Processing	48
2.7 Determining the Plasma Arc Radius	50
2.8 Review of Torch Speed vs. Plasma Flow Rate	52
2.9 Important Software Commands	54
Chapter 3: Experimental Results and Discussion	57
3.1 Inadequacy of DCEP Data During VPPAW	57
3.2 Curve Fitting of Data	60
3.3 Effect of Welding Current on the Arc Radius	67
3.4 Effect of Welding Mode on the Arc Radius	72
3.5 Effect of Shield Gas Composition on the Arc Radius	76
Chapter 4: Experimental Conclusions	80
References	81
Appendices	84
Appendix A	85
Appendix B	87
Appendix C	89

Appendix D	90
Appendix E	91
Curriculum Vitae	92

PREVIEW

LIST OF TABLES

Table 1: Table of thermal conductivity values of copper	37
Table 2: Table of values which control the daughterboard sampling frequency	56
Table 3: Table of values of the gain variable in the program RM7.BAS	56
Table 4: Table showing the welding parameters used in determining the effect of current changes on the plasma arc diameter	67
Table 5: Table showing the experimental welding parameters used in comparing the arc radii of variable polarity data vs. DCEN data	72
Table 6: Table of welding parameters used to test the effects of shield gas composition on the plasma arc diameter	76

LIST OF FIGURES

Figure 1: Diagram showing the dimensional differences between GTAW and PAW	6
Figure 2: Diagram showing DCEN and DCEP cycles in VPPAW	10
Figure 3: Photo of aluminum welded in VPPAW mode	11
Figure 4: Model of ion sputtering cleaning mechanism	16
Figure 5: Model of dielectric breakdown as a cleaning mechanism	17
Figure 6: Diagram of split anode setup	23
Figure 7: Cross-sectional view of copper anodes	24
Figure 8: Plot of current intensity vs. radial distance for three currents	25
Figure 9: Schematic drawing of the welding setup used for experiments	30
Figure 10: Photo of micrometer mounted on the torch	31
Figure 11: Schematic of full arc length	32
Figure 12: Calibration graph showing plasma gas flow rate vs. voltage	33
Figure 13: Calibration graph showing shield gas flow rate vs. voltage	34
Figure 14: Dimensions of the copper anode used in the split anode experiments	38
Figure 15: Photo of copper anode used in split anode experiments	39

Figure 16: Diagram showing the relative positions of the anodes and torch	41
Figure 17: Schematic of daughterboard configuration including jumper positions	44
Figure 18: Diagram showing the difference between bipolar and unipolar settings on the daughterboard	45
Figure 19: Graph of the welding signal with 200 μ F capacitor	46
Figure 20: Plot of typical VPPA data train taken from split anode experiments	51
Figure 21: Plot of welding current vs. torch travel distance of VPPAW data train	58
Figure 22: Diagram of torch and anodes during DCEP mode	59
Figure 23: Plot of relative intensity vs. travel distance for VPPA data	63
Figure 24: Plot of relative intensity vs. travel distance for VPPA data that has been symmetrized	64
Figure 25: Plot of welding current vs. travel distance for symmetrized data comparing 3rd, 5th and 7th order polynomials	65
Figure 26: Plot of current density vs. arc radius for three different polynomial functions of the same data train	66
Figure 27: Plot of arc radius vs. welding current for three orifice tips	70

Figure 28: Plot of ratio of arc diameter/orifice tip diameter as a function of linear plasma flow rate	71
Figure 29: Plot of arc radius vs. welding current for two different welding modes	74
Figure 30: Graph of Pang's [12] data showing how the arc temperature changes during VPPA welding	75
Figure 31: Photographs showing expansion of the arc under varying shield gas compositions	78
Figure 32: Plot of arc radius vs. shield gas composition for different orifice tips	79

CHAPTER 1: INTRODUCTION

1.1 WELDING ALUMINUM

Aluminum is the most common metal in the earth's crust, is cosmetically attractive, is lightweight, offers inherent corrosion resistance to many environments, and can be engineered to several specific applications. The methods used to join aluminum are mechanical means, adhesives, brazing and welding to mention a few. Of these, welding is most important in the aerospace industry. Aluminum's high thermal conductivity does not lend itself easily to many welding processes however, which means welding processes have to be carried out at relatively high heat inputs and fast weld travel rates [1]. In addition, welding aluminum and its alloys is made difficult because of its strong affinity for oxygen. This tenacious oxide layer is virtually impenetrable by usual thermal welding processes. Previous thermal welding processes relied on the use of corrosive fluxes to chemically combine with the aluminum oxide and form a fusible slag that was easily removed.

The melting temperature of aluminum oxide is 2310 K--more than two times the melting temperature of pure aluminum. Aluminum has a typical oxide layer of roughly 50-100 Å (even freshly scraped aluminum quickly forms a ~15Å oxide layer) [2]. The presence of aluminum oxide during the welding sequence tends to disrupt the solidification process thus rendering the weld pool susceptible to gas

contamination which in turn leads to such discontinuities as porosity and hot cracking [3-6, 10]. Solid aluminum oxide in the weld pool also leads to decreased ductility, lack of fusion, undercutting and irregular welds [6]. Hydrocarbons in particular are a problem because they are easily adsorbed on the porous oxide and later break down during the welding process to provide a source of hydrogen. Though hydrogen is only slightly soluble in solid aluminum, it is extremely soluble in molten aluminum and upon solidification, becomes entrapped in the weld bead.

PREVIEW

1.2 Gas Tungsten Arc Welding

Gas tungsten arc welding (GTAW) is presently used to join most aluminum alloys. GTAW is used to weld many types of alloys in all positions and weld complex shapes as well. GTAW uses a nonconsumable, 2% thoriated tungsten electrode. Thoria in the tungsten electrode gives rise to greater resistance to contamination, better current carrying capacity and easier arc starting [7]. Unlike other thermal welding processes, there is no need to use slag to protect the weld pool from atmospheric contamination since welding is performed in an inert environment of a shielding gas (usually argon) [8].

The disadvantage of GTAW when welding aluminum was that it required multiple passes to weld thick sections which meant increased time and cost. Workpiece distortion (i.e. waviness in elevation of the weldment and the surrounding metal called peaking) was evident because of the slow welding speeds used and therefore required corrective measures. The process was subject to slow deposition rates when welding with filler material. The welding event also had to be followed by costly, radiography testing to ensure 100% defect-free welds when welding critical parts. To obtain welds of good quality, it was essential that all surfaces to be welded and adjacent areas be clean.

1.3 Plasma Arc Welding

Plasma arc welding (PAW) is similar to GTAW in that they both use a nonconsumable tungsten electrode and both use a shielding gas to protect the electrode and weld pool from contamination. A schematic diagram comparing the two welding processes is shown in fig. 1.

PAW and GTAW differ in some important aspects. PAW uses a constricting orifice tip to concentrate the plasma arc into a more narrow column. The orifice tip covers the electrode and prevents it from contacting the surface of the workpiece whereas GTAW was subject to electrode contamination due to the small separation between it and the workpiece [7].

Aside from the shield gas, the plasma arc process also includes a second gas (usually argon) exclusively for the creation of the plasma. As the plasma gas is directed through the orifice tip, it is collimated into a narrow, concentrated plasma arc column. High temperatures are achieved that can not be achieved through GTAW. Several advantages over GTAW arise from this:

- 1.) an arc column has a small "footprint" radius,
- 2.) greater arc stability, less arc "wandering",
- 3.) higher heat concentration, less workpiece distortion, and
- 4.) greater workpiece penetration is achieved so keyhole mode welding is possible.

Due to the high power density created with the PAW process, PAW is especially useful for welding thick sections of aluminum up to 5/8 inch thick in a single pass whereas the GTAW process can only sufficiently weld aluminum sections 3/8 inch thick in a single pass.

PREVIEW

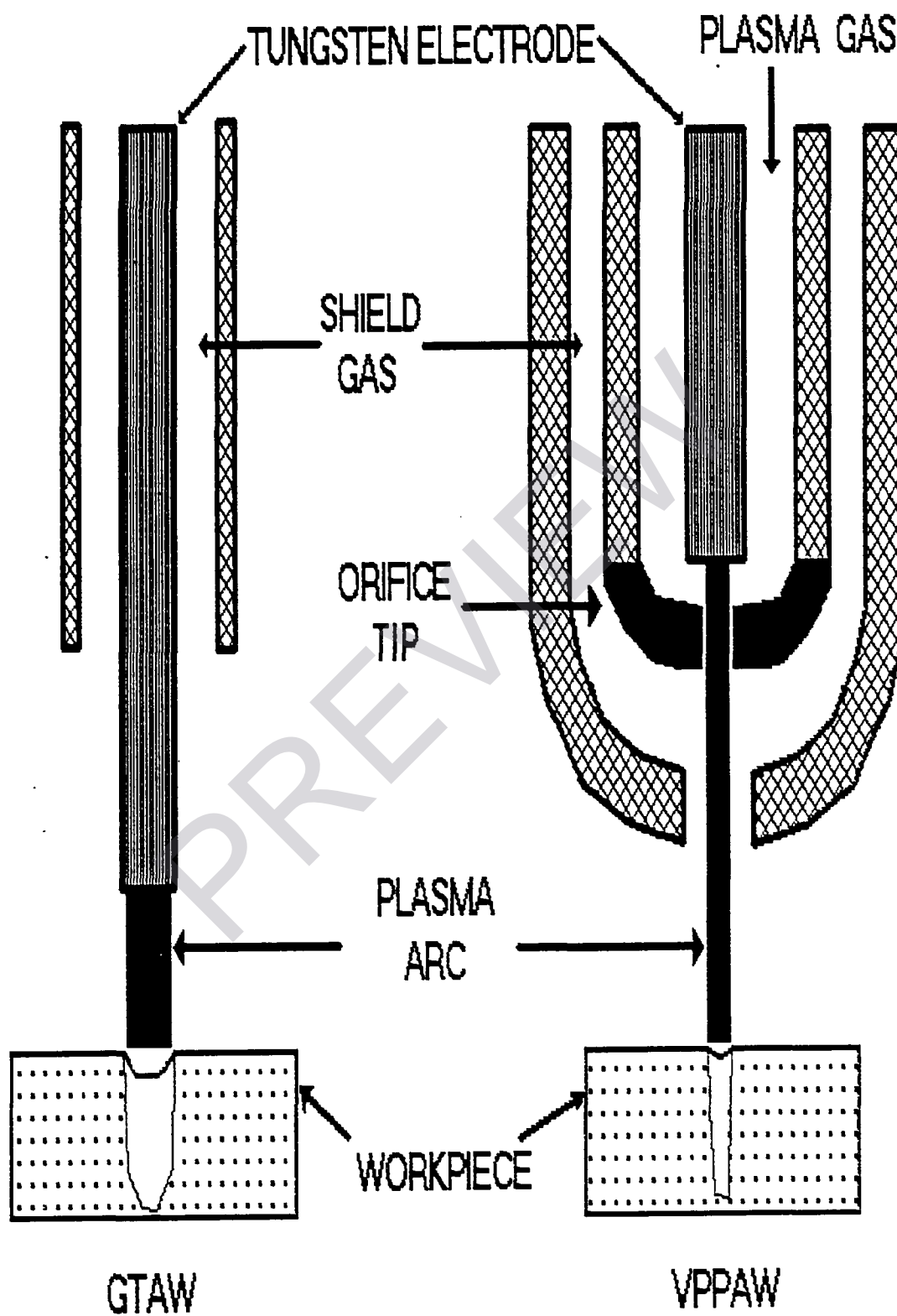


Figure 1: Diagram showing the dimensional differences between GTAW and PAW.

1.4 VARIABLE POLARITY PLASMA ARC WELDING

Variable polarity plasma arc welding (VPPAW) dates back to the plasma arc torch originally introduced by Linde Air Products in 1955. Ensuing efforts (notably by Bernard Van Cleave of the Boeing Co. [9]) sought to combine variable polarity with the successful plasma arc process. That is, to switch the polarity of the cathode and anode at a rapid rate. The technology of the time limited the success of the VPPAW process.

VPPAW is a very complex process and only the more pertinent components will be discussed here. The VPPAW process incorporates an asymmetric current waveform which consists of a positive cycle and a negative cycle as illustrated in fig. 2. During the positive cycle, the electrode is negative and the workpiece (the anode) is positive. This is known as Direct Current Electrode Negative or DCEN. During the negative cycle, the electrode is made positive and the workpiece is negative. This is known as Direct Current Electrode Positive or DCEP. The waveform is typically 20 milliseconds (msec) in the DCEN mode and 4 msec in the DCEP mode in order to achieve a balance between the high heating capability of the DCEN cycle and the cleaning feature of the DCEP cycle [10].

During the DCEN cycle, the electrons in the plasma arc accelerate and transfer their kinetic energy and work function to the workpiece and cause heating. The electrons carry most of the energy since they are quickly accelerated within the plasma arc column. During the DCEP cycle, the much larger plasma ions move

more slowly in the arc and do not contribute very much to heating the workpiece. Schoeck [11] calculated mobilities of electrons and argon ions in a plasma taking into account motion due to drift, diffusion and hydrodynamic flow and found that the mobility of the electron was 100 times higher than the argon ion.

During the DCEP cycle, the positively charged gas ions are accelerated towards the workpiece where they take part in a "cleaning" operation that is not fully understood and will be discussed in more detail later in the chapter. The result of the DCEP cycle is quite convincing--the removal of the tough aluminum oxide film is realized thus exposing the aluminum metal to the heat source. A photo of the cleaned area around a VPPA aluminum weld is shown in fig. 3. Note the "cleaned" areas in the vicinity ahead and to the sides of the weld bead. This is very important because the performance and reliability of the process is enhanced due to the insensitivity to the cleanliness of the workpiece surface. Pang [12] performed spectroscopic studies on contamination levels of hydrogen and oxygen during VPPAW of aluminum 2219 and 6061 and found contaminant amounts were not significantly altered by different levels of initial workpiece cleanliness. Nunes *et al.* [10] found that the procedures of cleaning surfaces by scraping and draw filing could be eliminated by using VPPAW instead of GTAW.

The VPPAW process is capable of welding in either cover pass mode or keyhole mode. In cover pass mode, there is an incomplete penetration of the workpiece whereas in keyhole mode welding there is a complete penetration of the

workpiece. Welding in the coverpass mode is usually reserved for second passes in which filler material is used to complete the joining process. When welding in keyhole mode, contaminant gases in the arc and weld pool are allowed to escape through the backside of the workpiece thus preventing entrapment of contaminants during the weld pool solidification process [13]. Welding in keyhole mode also prevents heat buildup in the workpiece because a portion of the energy is lost through the backside of the keyhole. Nunes *et al.* [10] found a significant reduction in peaking when using VPPAW as opposed to GTAW. Depeaking costs were reduced appropriately.

NASA uses VPPAW on the Space Shuttle External Tank and welds over 36,000 inches 2219 aluminum alloy up to 1 in thick on each tank without a single internal defect. No other welding process approaches this success.

PREVIEW

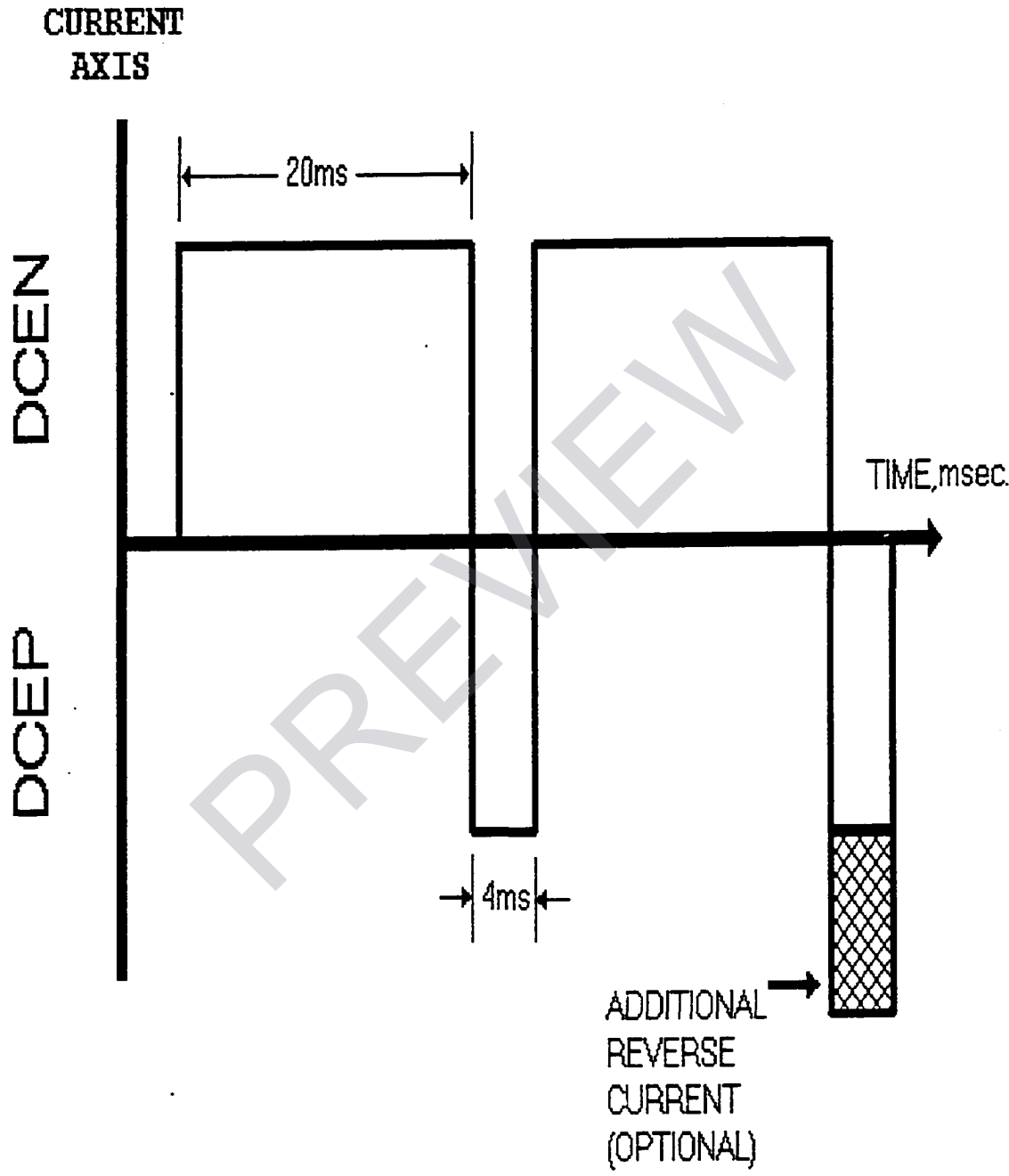


Figure 2: Diagram showing DCEN and DCEP cycles in VPPAW.



Figure 3: Photo of VPPA aluminum weld. Note the cleaned area around the weld bead.